Stress–strain–strain rate relation for the compressibility of sensitive natural clays

S. LEROUEIL,* M. KABBAJ,* F. TAVENAS* and R. BOUCHARD†

Four types of oedometer tests (constant rate of strain tests, controlled gradient tests, multiple-stage loading tests and creep tests) were carried out on a variety of Champlain sea clays. Results obtained on five sites are used to demonstrate that the rheological behaviour of these clays is controlled by a unique stress–strain–strain rate relationship. This relationship can be simply described by two curves (σ_p'–$\dot\varepsilon_v$ and (σ_v'/σ_p')–ε_v). The significance, the practical implications and the limitations of the model are also discussed.

Quatre types d'essais oedométriques (a vitesse constante de déformation, à gradient contrôlé, à chargement en plusieurs étapes et avec fluage) ont été effectués sur diverses argiles marines Champlain. Les résultats obtenus sur cinq sites sont utilisés pour démontrer que le comportement rhéologique de ces argiles est régi par une relation unique contrainte-déformation/vitesse de déformation. Cette relation peut être décrite de façon très simple par deux courbes (σ_p–$\dot\varepsilon_v$ et (σ_v'/σ_p')–ε_v). L'article analyse aussi la signification, les implications pratiques et les limitations du modèle.

NOTATION

C_c compression index
$C_{\alpha e}$ coefficient of secondary compression with respect to the void ratio
e void ratio
$\dot e$ $\partial e/\partial t$
E_{oed} oedometric modulus ($d\sigma_v'/d\varepsilon_v$)
H_0 initial height of the specimen
t time
u_b pore pressure at the base of the specimen
u_0 back pressure
α pore pressure distribution parameter
ε_v vertical strain ($\Delta H/H_0$)
$\dot\varepsilon_v$ $\partial\varepsilon_v/\partial t$
σ_v total vertical stress
σ_p' preconsolidation pressure
σ_v' vertical effective stress
$\dot\sigma_v'$ $\partial\sigma_v'/\partial t$

INTRODUCTION

One-dimensional consolidation has always been considered one of the most important geotech-

nical problems and it is not surprising that hundreds of papers have been written on this subject. Most of the studies are theoretical, analytical or numerical and more than 25 different rheological models have been suggested for clays. Simply, four families of rheological models can be defined: if e is the void ratio, σ_v' the vertical effective stress, t the time, $\dot e = \partial e/\partial t$ and $\dot\sigma_v' = \partial\sigma_v'/\partial t$ these families can be represented by the following equations.

$$R(\sigma_v', e) = 0 \tag{1}$$

$$R(\sigma_v', e, t) = 0 \tag{2}$$

$$R(\sigma_v', e, \dot\sigma_v, \dot e) = 0 \tag{3}$$

$$R(\sigma_v', e, \dot e) = 0 \tag{4}$$

Equation (1) is representative of models in which the effective stress–void ratio response of the soil is unique and independent of time or strain rate. This is the case for the classical Terzaghi theory of consolidation in which a linear effective stress–void ratio relation is assumed. The model suggested by Davis & Raymond (1965) based on a linear void ratio-logarithm of effective stress relation is also of this type. Although equation (1) is widely used in practice, it has been recognized ever since Buisman (1936) that the void ratio varies under a constant effective stress and thus that equation (1) is not sufficient to describe the rheological behaviour of clays completely. Koppejan (1948), Bjerrum (1967) and Hansen (1969) have proposed models represented by equation (2) in which the void ratio is a function of the effective stress and time. A major difficulty, however, is encountered with these models when an origin for time must be defined, particularly when the applied load varies with time.

The models corresponding to equations (3) and (4) overcome this difficulty since the behaviour of the material depends only on its present conditions and is not a function of previous history. Taylor & Merchant (1940) were the first to suggest a model of the type represented by equation (3) in which the rate of change in void ratio is a function of the effective stress, the void ratio and the rate of change in effective stress. This suggestion has been followed by

numerous researchers (Gibson & Lo, 1961; Wu, Resendiz & Neukirchner, 1966; Poskitt & Birdsall, 1971; Sekiguchi & Toriihara, 1976). Models corresponding to equation (4) show a unique relationship between the effective stress, the void ratio and the rate of change in void ratio; they can be represented in an $e-\sigma_v'$ diagram by $\dot{e}$ = constant lines called isotaches by Šuklje (1957, 1969a). Various equations have been suggested to define these isotaches. The first and also the simplest corresponds to Taylor's theory B (1942)

$$\dot{e} = a\sigma_v' + be + c \qquad (5)$$

Other more complex equations have been suggested by Barden (1965), Šuklje (1969b), Poorooshasb & Sivapatham (1969), Battelino (1973) and Hawley & Borin (1973).

The rheological models proposed were seldom assessed experimentally or only on the basis of a few laboratory test results. Experimental studies, however, have been performed on natural clays (Crawford, 1965; Jarrett, 1967; Berre & Iversen, 1972; Sällfors, 1975; Larsson, 1981) and on resedimented clays (Smith & Wahls, 1969; Aboshi, 1973; Burghignoli, 1979), but in each study only one type of test was used: constant rate of strain (CRS) tests by Crawford (1965), Smith & Wahls (1969) and Sällfors (1975); constant rate of loading test by Jarrett (1967) and Burghignoli (1979); total load applied by steps by Berre & Iversen (1972) and Larsson (1981). It is thus difficult to obtain an overall view of the rheological behaviour of clays from these studies. As a result this abundant literature has modified neither the common practice based on the Terzaghi theory nor the way of thinking on clay behaviour.

About half a century after the work of Terzaghi (1923) and Buisman (1936) engineers are still undecided on whether there is a combination of primary and secondary compressions during primary consolidation of thick layers of clay. Šuklje (1957), Barden (1965) and Bjerrum (1967) have expressed the idea that there is a combination of both processes (theory B, from Ladd, Foott, Ishihara, Schlosser & Poulos, 1977), while Leonards (1977) and Ladd et al. (1977) think that secondary compression develops only after primary consolidation is completed ($\Delta u \approx 0$), (theory A from Ladd et al., 1977). Here again, the experimental evidence is almost non-existent or not convincing: the consolidation test results obtained by Berre & Iversen (1972) on specimens of different heights which are often used to validate theory B were also used by Leonards (1977) to justify theory A; the tests carried out by Aboshi (1973) on a remoulded clay indicate a behaviour somewhere in between the predictions of theories A and B.

Therefore it was decided to initiate a detailed research programme on consolidation. In the first stage, different types of oedometer tests (CRS tests, controlled gradient tests (CGTs), stage loading tests and long-term creep tests) were carried out on a variety of clays, and from these experimental data obtained on small specimens a rheological model has been developed. The objective of this Paper is to present these results. In the second stage of the research, the behaviour of clays observed in situ is compared with the behaviour observed in the laboratory; results in terms of the preconsolidation pressure have been published (Leroueil, Samson & Bozozuk, 1983; Leroueil, Tavenas, Samson & Morin, 1983; Morin, Leroueil & Samson, 1983). A detailed analysis of the stress–strain–strain rate behaviour of well-defined clay layers under three test embankments will be the subject of another paper.

CLAYS INVESTIGATED

The clays investigated were formed in the Champlain sea which occupied the St Lawrence lowlands and the Ottawa valley from approximately 12 500 to 10 000 Before Present. General physical and mechanical properties of these marine clays have been presented by Leroueil, Tavenas & Le Bihan (1983): the organic matter content is usually less than 1% and the sensitivity greater than 15. According to Lebuis, Robert & Rissmann (1982), less than 50% of the clay fraction is phyllosilicates and amorphous materials, the remainder being primary minerals, mainly quartz, plagioclase and potassium feldspar.

Eleven sites were investigated by Terratech Ltd, Montreal, and Laval University, Quebec, and 14 series of tests were carried out to study the preconsolidation pressure of the clays (Leroueil, Tavenas, Samson & Morin, 1983). The oedometer test data have been reanalysed in detail to extract the rheological behaviour of these clays (Kabbaj, Leroueil & Tavenas, 1984).

Typical results obtained for five representative sites are presented here. The main characteristics of the clays are shown in Table 1. The natural water content varies from 63% to 89%, the plasticity index ranges between 19 and 43, the liquidity index varies from 1·1 to 2·7 and the preconsolidation pressure measured in conventional oedometer tests ($\Delta\sigma_v/\sigma_v = 0\cdot5$ and a reloading schedule of 24 h) ranges from 88 kPa to 270 kPa.

Table 1. Average geotechnical properties of clays

Site	Depth: m	Water content:* %	w_L	I_p	I_L	Clay fraction	S_t (fall-cone)	c_u (field vane)	σ'_{v0}: kPa	$\sigma'_{p(conv)}$: kPa
Batiscan	7·3	79·6 (73·8–84·9)	43	21	2·7	81	125	25	65	88
Joliette	6·7	65·0 (63·1–66·5)	41	19	2·3	54	96	29	40	115
Louiseville	9·2	76·5 (73·8–79·4)	70	43	1·1	81	28	45	58	160
Mascouche	3·8	67·6 (64·1–70·9)	55	30	1·4	77	65	70	34	270
St Césaire	6·8	84·8 (82·4–89·0)	70	43	1·3	84	22	27	68	90

* Extreme values are given in parentheses.

TEST PROGRAMME AND EQUIPMENT

Various types of oedometer tests have been performed in this study

(a) Multiple-stage loading tests with a stress increment ratio $\Delta\sigma_v/\sigma_v = 0·5$ and reloading at the end of primary consolidation $((MSL)_p)$ or after 24 h $((MSL)_{24})$ (in this test, drainage was allowed only at the top of the specimen and the pore pressure was measured at the bottom).

(b) CRS tests (Smith & Wahls, 1969; Wissa, Christian, Davis & Heiberg, 1971)

(c) CGTs in which the pore pressure difference Δu_b between the top and the bottom of the specimen was maintained constant (Lowe, Jonas & Obrician, 1969)

(d) Creep tests in which the specimen was first loaded step by step to an initial stress equivalent to the in situ effective vertical stress; then, it was loaded in one step to the final stress and maintained under this stress for more than 70 days.

In CRS tests and CGTs, the average strain $\varepsilon_v = \Delta H/H_0$ or the void ratio e can be related to an average effective stress calculated with the following equation

$$\sigma_v' = \sigma_v - u_0 - \alpha(u_b - u_0) \qquad (6)$$

where σ_v is the total vertical applied stress, u_0 is the applied back pressure and u_b is the pore pressure measured at the base of the specimen. Smith & Wahls (1969) and Wissa et al. (1971) suggested a value of 0·67 for α. Although the value is in agreement for low values (below 0·4) of $du_b/d\sigma_v$, Janbu, Tokheim & Senneset (1981) have indicated slightly higher values of α when $du_b/d\sigma_v$ becomes higher ($\alpha = 0·70$ for $du_b/d\sigma_v = 0·7$; $\alpha = 0·75$ for $du_b/d\sigma_v = 0·92$). The α values used in this study were those suggested by Janbu et al.

Since the aim of the study was to determine the rheological behaviour of natural clays, it was first necessary to analyse the eventual influence of the rate of increase of the vertical effective stress $\dot{\sigma}_v' = \partial\sigma_v'/\partial t$. To do so, it was decided to carry out, on the clay from Batiscan, CRS tests in which there is a constant $\dot{\varepsilon}_v = \partial\varepsilon_v/\partial t$ and a continuous increase in σ_v', and creep tests in which σ_v' is constant and thus $\dot{\sigma}_v' = \partial\sigma_v'/\partial t$ is equal to zero after the end of pore pressure dissipation (Bouchard, 1982).

On the clay from St Césaire, three CRS tests, three CGTs and one $(MSL)_p$ test were carried out (Samson, Leroueil, Morin & Le Bihan, 1981). The results obtained on this clay, and those obtained on the clay from Batiscan, are presented in detail in this Paper.

On the three other clays selected (Joliette (Samson et al., 1981); Louiseville and Mascouche (Leahy, 1980)), 3–6 CRS tests, one CGT and up to two multiple-stage loading tests were carried out. Only reduced data are presented.

The 200 mm dia. Laval sampler (La Rochelle, Sarrailh, Tavenas, Roy & Leroueil, 1981) was used on the sites from Batiscan, Louiseville and Mascouche and the samples were stored in a humid room at 8 °C. All the tests on the clays from these sites were performed at Laval University, Quebec. Except for the CGTs, all the oedometer tests were performed without back pressure on specimens 19·0 mm high and 50·8 mm in diameter. The CGTs were carried out in a specially designed cell (Samson et al., 1981) in which a back pressure of 100 kPa was applied at the top of the specimen. The specimens were 15 mm high and 55 mm in diameter. For all these tests, synthetic filter cloth of low compressibility and high durability was installed at the top and the bottom of the specimen.

On the St Césaire and Joliette sites the clay was sampled with a modified 70 mm dia. Geonor piston sampler with an area ratio of 11% and samples were stored in a humid room at 10 °C. The tests were performed by Terratech
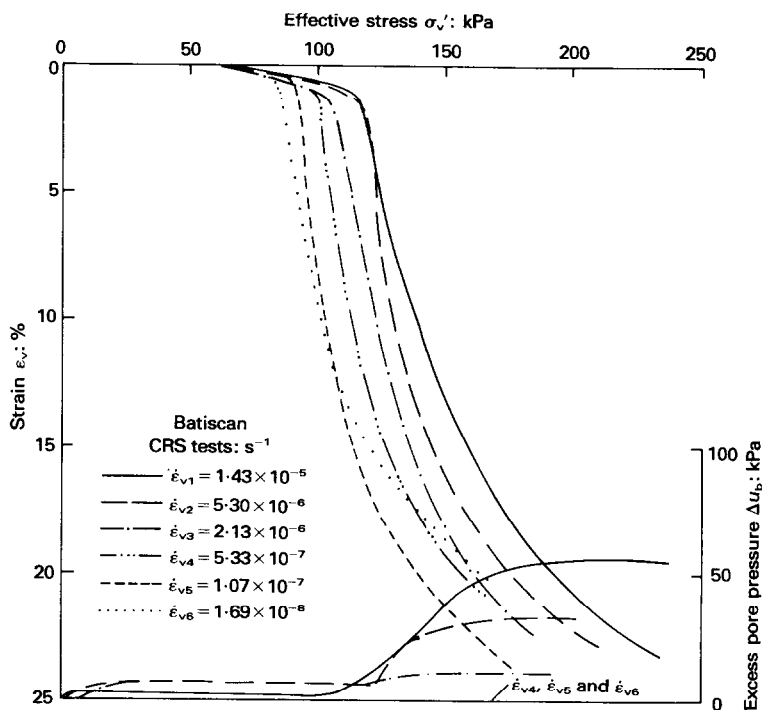
Fig. 1. Typical CRS oedometer tests on Batiscan clay

Ltd, Montreal, with cells (Samson *et al.*, 1981) in which a back pressure of 100 kPa was applied at the top of the specimen and the pore pressure was measured at the base. The specimens were also 15 mm high and 55 mm in diameter.

In all tests, the vertical displacements measured were corrected for the filter papers and system compressibility. Because of the natural variability of the initial void ratio, even if it was small for the clays considered, all the test results were interpreted in terms of strain ε_v rather than in terms of void ratios.

RHEOLOGICAL BEHAVIOUR OF NATURAL CLAYS

Clay from Batiscan

Batiscan is situated on the north shore of the St Lawrence River, about 110 km west of Quebec City. The clay tested was taken at a depth of 7·25–7·46 m. The water content is about 80%, the plasticity index 21 and the liquidity index 2·7. The preconsolidation pressure, as determined from a conventional oedometer test, is 88 kPa (Table 1).

Eighteen CRS tests were carried out with the strain rate varying from test to test between

$1·7 \times 10^{-8} \, \text{s}^{-1}$ and $4 \times 10^{-5} \, \text{s}^{-1}$. Typical results are presented in Fig. 1 where the origin of strain is taken at $\sigma_v' = 65$ kPa, a stress equal to the vertical effective stress in the field at the depth of the specimens. This choice has only been made to be able to compare CRS tests results with the creep tests in which the clay was first loaded to σ_{v0}' and settlement measurements started from this state. Fig. 1 shows that, the higher the strain rate, the higher the pore pressure increase at the base of the specimen and that, for strain rates lower than $5 \times 10^{-7} \, \text{s}^{-1}$, the excess pore pressure is so small that it cannot be measured. It is also shown that, at a given strain, the higher the strain rate, the higher the effective stress, which is consistent with observations by Crawford (1965), Sällfors (1975) and Leroueil, Samson & Bozozuk (1983). It should be noted, however, that the $\dot{\varepsilon}_{v6}$ curve intersects the other curves significantly; among the 18 tests, three have shown such behaviour and they will be discussed later.

Nine creep oedometer tests were also carried out on this clay. The final stresses varied between 67 kPa and 151 kPa. The results, which are shown in Fig. 2, are consistent with earlier observations (Leonards & Girault, 1961; Bjerrum, 1967; Leroueil, 1977). For high stress in-
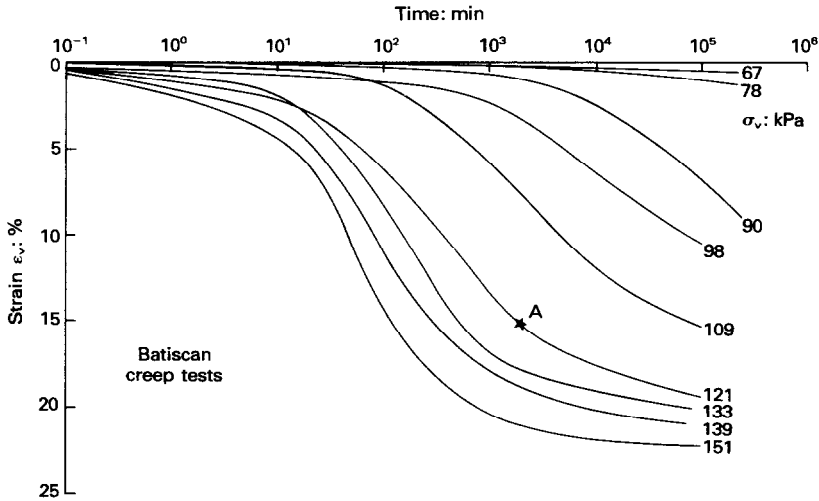
Fig. 2. Creep oedometer tests on Batiscan clay

creases, the ε_v–log t curves have a typical S shape; however, for small stress increases, the curves have a continuously increasing slope with time. The same results are also shown in Fig. 3 in an ε_v–log $\dot{\varepsilon}_v$ diagram.

At the beginning of the test, there were excess pore pressures and the effective stresses were smaller than the applied stresses. Unfortunately, since pore pressures were not measured in these tests, the effective stresses were unknown. However, from the shape of the curves shown in Figs 2 and 3 and from experience with other clays, it is thought that the excess pore pressures are small and the effective stress is approximately equal to the applied stress when $\dot{\varepsilon}_v \leqslant 10^{-6}\,\text{s}^{-1}$.

The curves shown in Fig. 3 can thus be considered as ε_v–$\dot{\varepsilon}_v$ relationships under constant effective stress when $\dot{\varepsilon}_v \leqslant 10^{-6}\,\text{s}^{-1}$.

It is worth noting the shape of these ε_v–$\dot{\varepsilon}_v$ curves, particularly those obtained for stresses of 90 kPa, 98 kPa and 109 kPa. There is first a rapid decrease in the strain rate at low strains followed by an approximately constant strain rate with the strain increasing between 1% and 3% (a strain corresponding to the passing of σ_p' in CRS tests, Fig. 1). At higher strains, the strain rate decreases progressively.

From the creep test results, it is possible to define effective stress–strain relations for strain rates $\dot{\varepsilon}_v$ of $10^{-6}\,\text{s}^{-1}$, $10^{-7}\,\text{s}^{-1}$, $10^{-8}\,\text{s}^{-1}$ and even
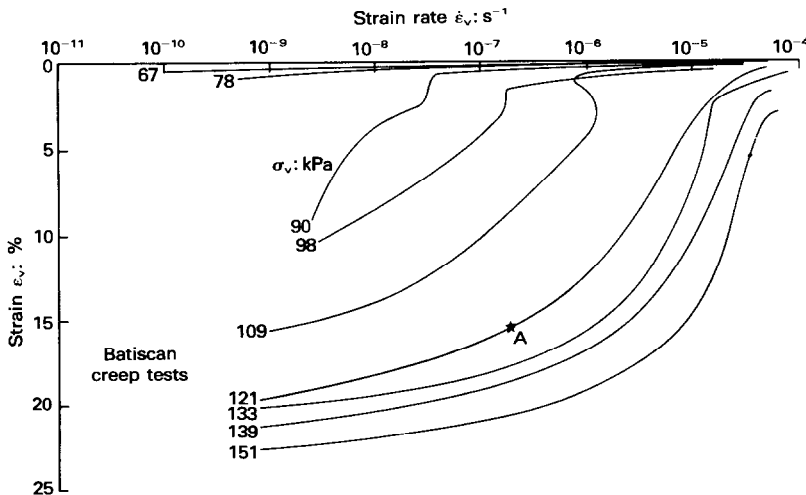
Fig. 3. Strain–strain rate variation for creep tests on Batiscan clay

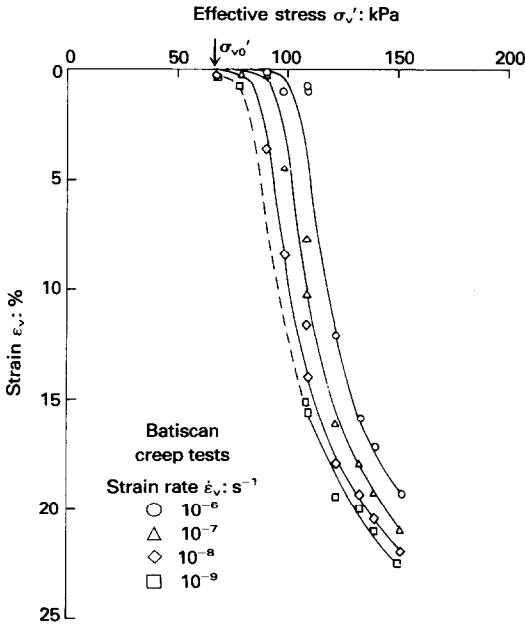**Effective stress σ_v': kPa**

Fig. 4. Constant $\dot{\varepsilon}_v$ curves deduced from creep tests on Batiscan clay

$10^{-9}\,\text{s}^{-1}$. This is done in Fig. 4 and it can be seen that these curves are very similar in shape and position to the ones observed in CRS tests (Fig. 1).

From the two sets of curves presented in Figs

1 and 4, it is evident that the strain rate is a very important factor influencing the rheological behaviour of Batiscan clay. It is important to know which of equations (3) and (4), or in terms of strains the equations

$$R'(\sigma_v', \varepsilon_v, \dot{\sigma}_v', \dot{\varepsilon}_v) = 0 \tag{7}$$

$$R'(\sigma_v', \varepsilon_v, \dot{\varepsilon}_v) = 0 \tag{8}$$

is representative of the clay behaviour.

In the CRS tests $\dot{\varepsilon}_v$ is constant and the effective stress is continuously increasing, while in the creep tests σ_v' is constant (for $\dot{\varepsilon}_v \leqslant 10^{-6}\,\text{s}^{-1}$) and thus $\dot{\sigma}_v' = 0$. Therefore, any effect of σ_v' should be clearly identified from the test results. To analyse this point, the effective stresses obtained in the various tests at strains of 5%, 10%, 15% and 20% are plotted against the strain rate in Fig. 5. At strains of 5%, 10% and 15%, well-defined $\dot{\varepsilon}_v$–σ_v' relations, independent of the test used, are found, indicating that the rate of increase in effective stress $\dot{\sigma}_v'$ has no influence on the rheological behaviour of clays and that there is a unique σ_v'–ε_v–$\dot{\varepsilon}_v$ relationship for this clay.

At a strain of 20%, the scatter is important: for example, at a strain rate of $1 \cdot 07 \times 10^{-7}\,\text{s}^{-1}$, one CRS test gives an effective stress that is 12 kPa in excess of the average curve while another gives an effective stress that is 14 kPa below this curve. For CRS tests with strain rates of $1 \cdot 7 \times 10^{-8}\,\text{s}^{-1}$ and $3 \cdot 6 \times 10^{-8}\,\text{s}^{-1}$ the effective stresses are significantly higher than the effective
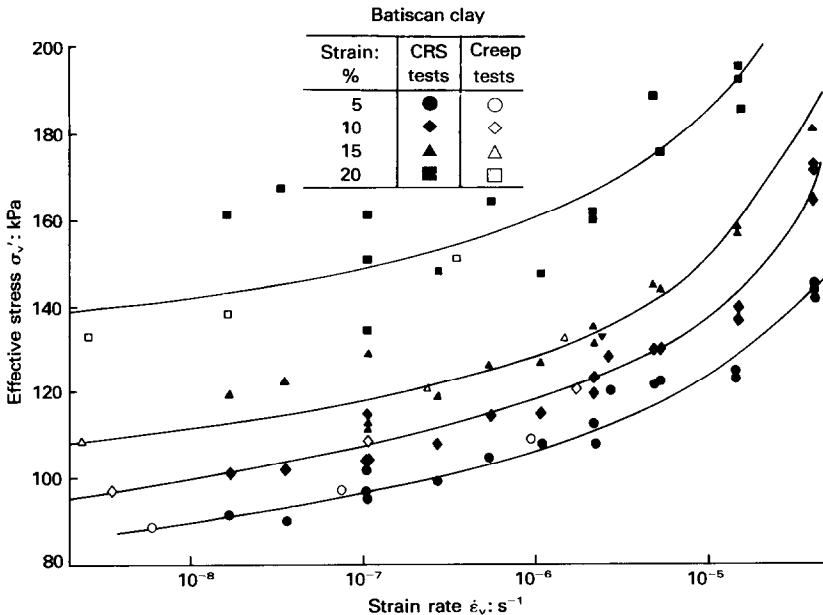
Batiscan clay

Fig. 5. Effective stress–strain rate variation at various strains for Batiscan clay

stresses deduced from creep tests. It is difficult to say whether the scatter (or differences) observed at 20% strain is due to fundamental rheological clay behaviour or to the natural variability of the specimens. This latter possibility is real, as small variations in grain size distribution, water content and particle arrangement have a significant influence on the stress necessary to compress the soil at high strains. However, for strains up to 15% and strain rates usually encountered in the laboratory, it can be considered that there is a unique stress–strain–strain rate relationship, independent of the rate of effective stress change.

The existence of such a $\sigma_v'-\varepsilon_v-\dot{\varepsilon}_v$ relationship has been confirmed by two special CRS tests in which the strain rates were changed at various strains. The test SP1 (Fig. 6) started with a strain rate $\dot{\varepsilon}_{v1} = 2\cdot7 \times 10^{-6}\,\mathrm{s}^{-1}$ up to a strain of 3·7%, then was switched to $\dot{\varepsilon}_{v2} = 1\cdot05 \times 10^{-7}\,\mathrm{s}^{-1}$ up to a strain of 7·2% and back again. The test SP2 began with a strain rate $\dot{\varepsilon}_{v2} = 1\cdot05 \times 10^{-7}\,\mathrm{s}^{-1}$ up to $\varepsilon_v = 4\cdot5\%$, then was switched to $\dot{\varepsilon}_{v1}$ up to $\varepsilon_v = 8\cdot8\%$ and back again. A strain rate $\dot{\varepsilon}_{v3} = 1\cdot3 \times 10^{-5}\,\mathrm{s}^{-1}$ was also used for the SP2 test at strains between 17·7% and 21·8%. The results in Fig. 6 clearly show that there is a unique stress–strain–strain rate relationship for this clay, at least for strains less than 16%. At strains larger than 23%, the two $\dot{\varepsilon}_{v1}$ curves are different, probably because of small differences in the specimens. However, the results prove that there is still a strain rate effect at strains as high as 23%. Graham, Crooks & Bell (1983) also observed such strain rate effects at large strains on a clay from Belfast.

From the stress–strain curves presented in Figs 1 and 4, it can be observed that the strain on passing the preconsolidation pressure σ_p' is about 1% for all the tests. A $\sigma_p'-\dot{\varepsilon}_v$ relationship can thus be determined in the same manner as that by which $\sigma_v'-\dot{\varepsilon}_v$ curves were established at other strains (Fig. 5). Both series of $\sigma_p'-\dot{\varepsilon}_v$ points deduced from CRS (Fig. 1) and creep tests (Fig. 4) and plotted in Fig. 7 are on the same average curve.

The $\sigma_v'-\dot{\varepsilon}_v$ and $\sigma_p'-\dot{\varepsilon}_v$ curves presented in Figs 5 and 7 have roughly the same shape and it appeared that the complete $\sigma_v'-\varepsilon_v-\dot{\varepsilon}_v$ relationship for the clay could be normalized. This was verified in the following way: for CRS tests, the vertical effective stress σ_v' was normalized with respect to the preconsolidation pressure $\sigma_p'(\dot{\varepsilon}_v)$ associated with the corresponding strain rate on the average curve (Fig. 7). The $\sigma_v'/\sigma_p'(\dot{\varepsilon}_v)$ ratios were plotted against ε_v for the 18 tests (Fig. 8). Fourteen normalized test curves for strain rates between $1\cdot4 \times 10^{-5}\,\mathrm{s}^{-1}$ and $1\cdot07 \times 10^{-7}\,\mathrm{s}^{-1}$ fall in
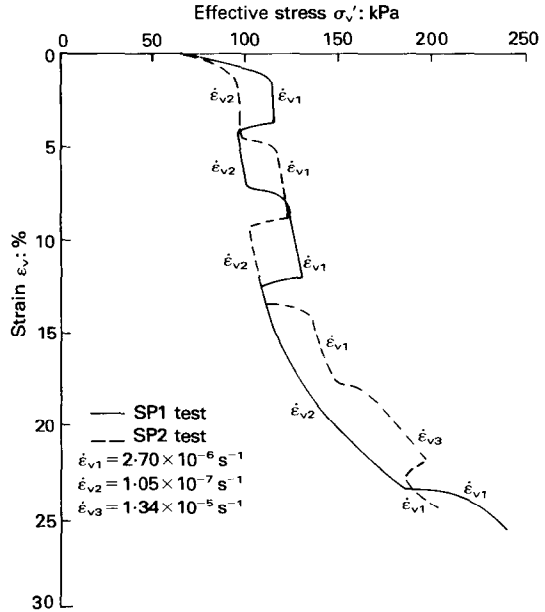

Fig. 6. Special CRS oedometer tests on Batiscan clay

a narrow range, while four are out of this range and will be discussed later. For the creep tests, the strain rate varied continuously during the test, but at a given strain there was a definite strain rate and it was possible to normalize the effective stress (equal to the applied stress when $\dot{\varepsilon}_v < 10^{-6}\,\mathrm{s}^{-1}$) with respect to the preconsolidation pressure associated with the strain rate at that strain (Fig. 7). For example, if we consider the creep test in which $\sigma_v = 121\,\mathrm{kPa}$ is applied, after 2000 min the strain is equal to 15·5% (Fig. 2, point A), the strain rate of the specimen at that moment is $2 \times 10^{-7}\,\mathrm{s}^{-1}$ (Fig. 3, point A) and the preconsolidation pressure σ_p' corresponding to this strain rate is 94 kPa (Fig. 7, point A). It is then possible to plot $\sigma_v'/\sigma_p'(\dot{\varepsilon}_v)$ (121/94 = 1·29) against $\varepsilon_v = 15\cdot5\%$ (Fig. 9, point A). All the creep tests were interpreted in this way and the results are plotted in Fig. 9.

As for the CRS tests (Fig. 8), with the exception of the two more rapid tests carried out with a strain rate of $4\cdot0 \times 10^{-5}\,\mathrm{s}^{-1}$, they all fall in a very narrow range up to strains of 15%. At larger strains, the range obtained with 14 tests enlarges and, moreover, the two slowest CRS tests ($\dot{\varepsilon}_v = 3\cdot6 \times 10^{-8}\,\mathrm{s}^{-1}$ and $1\cdot7 \times 10^{-8}\,\mathrm{s}^{-1}$) go out of this range. There are two possible reasons for the behaviour in these two tests: the first is associated with the natural variability of the specimens; the second is associated with a thixotropic hardening of the clay skeleton at very small strain rates of the type observed by Leonards &
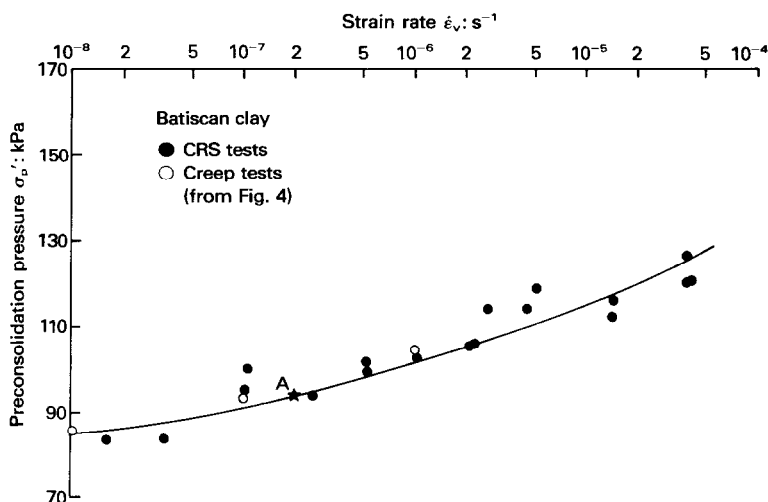
Fig. 7. Variation in preconsolidation pressure with strain rate for Batiscan clay

Altschaeffl (1964). No definite answer can be given and this point will need more consideration in future comparisons between $\sigma_v'-\varepsilon_v-\dot{\varepsilon}_v$ relationships in the laboratory and in situ. The two more rapid CRS tests give normalized curves which are markedly different from the others; in particular, they are less steep. During these tests, the pore pressures measured at the bottom of the specimens were very high with $\Delta u_b/\Delta\sigma_v$ values as high as 0·89 and the method of interpretation is probably doubtful under these conditions. Another explanation arises

from a different viscous behaviour of the clay at very high strain rates. Such normalized stress–strain curves with a different shape have been observed on other clays.

Considering now the creep tests (Fig. 9), all the normalized data fall within the range obtained from the 14 CRS tests; even at the slow strain rate of $10^{-8}\,\mathrm{s^{-1}}$ (circled points), the data points are well in the middle of the range. Thus,
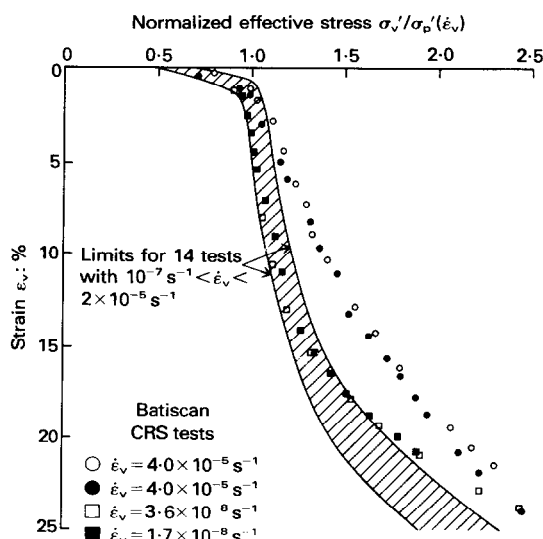

Fig. 8. Normalized effective stress–strain relationship deduced from CRS oedometer tests on Batiscan clay
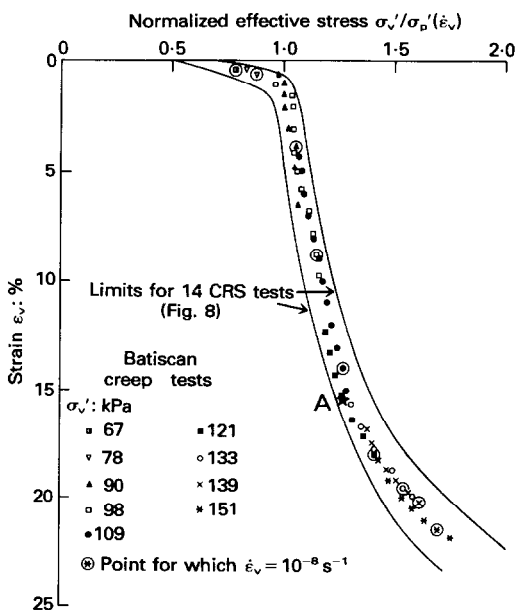

Fig. 9. Normalized effective stress–strain relationship deduced from creep oedometer tests on Batiscan clay

it can be concluded that for all the creep and CRS tests, with the exception of those carried out at very high strain rates and in which the pore pressure is high (and possibly with the exception of those carried out at slow strain rates when at large strains), for Batiscan clay there is a unique stress–strain–strain rate relationship which can be normalized and represented by only two curves: σ_p'–$\dot{\varepsilon}_v$ and $\sigma_v'/\sigma_p'(\dot{\varepsilon}_v)$–$\varepsilon_v$.

Clay from St Césaire

The site of St Césaire is located in the Champlain sea basin, about 50 km south east of Montreal. The clay specimens used for this study were taken at a depth of 6·55–7·04 m. They are characterized by an average water content of 85%, a liquid limit of 70, a conventional pre-consolidation pressure of 90 kPa and a sensitivity of 22 (Table 1).

Three CRS tests were carried out at strain rates of $2 \cdot 2 \times 10^{-5} \, \mathrm{s}^{-1}$, $4 \cdot 5 \times 10^{-6} \, \mathrm{s}^{-1}$ and $6 \cdot 67 \times 10^{-7} \, \mathrm{s}^{-1}$. The results are shown in Fig. 10. At a strain rate of $6 \cdot 67 \times 10^{-7} \, \mathrm{s}^{-1}$, the excess pore pressure is negligible. However, at a strain rate of $2 \cdot 2 \times 10^{-5} \, \mathrm{s}^{-1}$, the excess pore pressure is high, with $du_b/d\sigma_v$ as high as 0·5. In the normally consolidated clay range, the strain rate

effect is very clear: at a given strain, the higher the strain rate, the higher is the effective stress.

Three CGTs were also carried out with constant pore pressure differences Δu_b between the top and the bottom of the specimen of 3·6 kPa, 15 kPa and 35 kPa. The corresponding stress–strain curves are shown in Fig. 11(a). The higher the pore pressure difference, the higher is the effective stress at a given strain. This is consistent with the results obtained from CRS tests since the higher the pore pressure difference the higher is the strain rate (Fig. 11(b)). Also shown on this figure is the fact that the strain rate reaches a maximum at a strain corresponding approximately to the passage of the preconsolidation pressure (3–5% for this clay sampled with a 70 mm dia. piston sampler) and then decreases.

One multiple-stage loading test ((MSL)$_p$) with a stress increment ratio $\Delta\sigma_v/\sigma_v = 0 \cdot 5$ and reloading at the end of primary consolidation (more precisely when $\Delta u_b \approx 1$ kPa) was also carried out. The average strain and the pore pressure measured at the base of the specimen for the 65–99 kPa, 99–149 kPa and 149–226 kPa loading steps are plotted as functions of the logarithm of time in Fig. 12. The end-of-loading points are plotted in a σ_v'–ε_v diagram (Fig. 13)
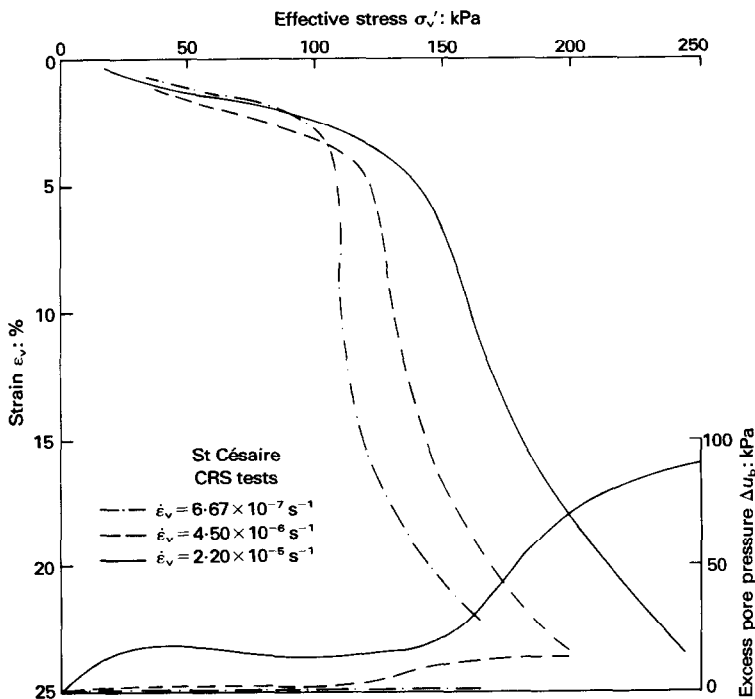

Fig. 10. CRS oedometer tests on St Césaire clay (after Samson et al., 1981)
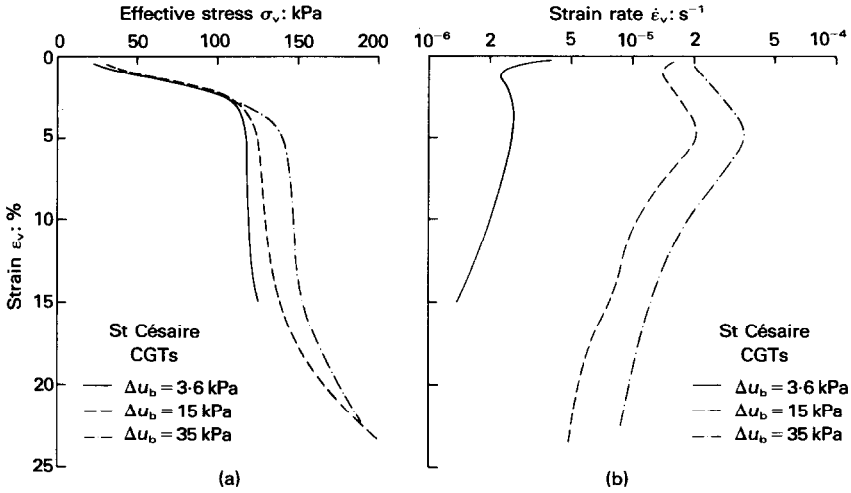
Fig. 11. Controlled gradient oedometer tests on St Césaire clay (after Samson *et al.*, 1981)
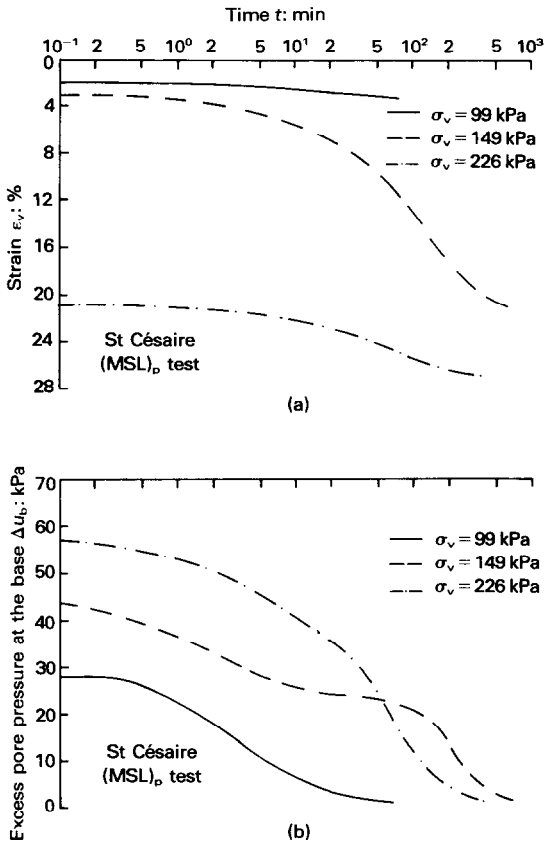

Fig. 12. Multiple-stage loading oedometer test on St Césaire clay (after Samson *et al.*, 1981)
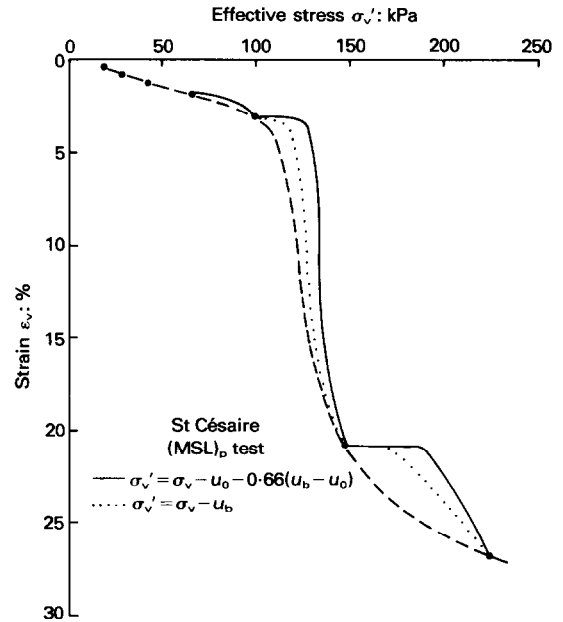

Fig. 13. Effective stress–strain curves deduced from multiple-stage loading oedometer tests on the St Césaire clay

and the classical oedometric curve (broken line) is drawn. Also shown in this figure with full lines are the stress–strain curves obtained from the data presented in Fig. 12 and a calculation of the average effective stress by using equation (6) with an α value of $0 \cdot 66$. This last calculation is not rigorous just after loading, when the excess pore pressure is high, but it gives a higher limit for σ_v'. An extreme lower limit is given by considering the effective stress at the base of the specimen: $\sigma_v' = \sigma_v - u_b$ (dotted line in Fig. 13). The difference between these two curves is relatively small and the error in the average effective stress calculated by using equation (6) is limited to a few kilopascals. The results shown in Figs 12 and 13 call for some remarks.

(a) The loading from 65 kPa to 99 kPa is typical of the behaviour of eastern Canadian overconsolidated clays. The duration of the primary consolidation is relatively short (Fig. 12(b)) and the ε_v–log t curve has a slope that increases continuously with time. The Δu_b–log t curve for loading from 99 kPa to 149 kPa is typical of a clay passing its preconsolidation pressure with a well-defined step between 10 and 60 min, as previously established by Leroueil, Le Bihan & Tavenas (1980). The accumulated strain (about 17%) during this step is very important. Finally, the behaviour observed during the loading from 149 kPa to 226 kPa is typical of a normally consolidated clay.

(b) Even if there is an eventual small error in the calculated average effective stress, the stress–strain curves shown in Fig. 13 are representative of the real behaviour. They are very different from the classical oedometric curve (broken line) showing, during the first phases of the loading, a rapid increase in the effective stress with small strains followed by a progressive increase in the effective stress with a significant accumulation of strain. Berre & Iversen (1972) observed similar behaviour in a Norwegian clay.

As for the clay from Batiscan, it is possible to verify for the clay from St Césaire whether there is a unique σ_v'–ε_v–$\dot{\varepsilon}_v$ relationship and whether this relationship can be normalized. To do so, it is first necessary to define the preconsolidation pressure–strain rate relation. For the CRS tests (Fig. 10), the preconsolidation pressures obtained at strains of 3–5% are plotted against the imposed strain rates in Fig. 14. In the CGTs, the strain rate is varying continuously (Fig. 11(b)). It is possible, however, to associate the preconsolidation pressure with the strain rate of the specimen when passing this preconsolidation pressure. This is done in Fig. 14 and it can be concluded that the σ_p'–$\dot{\varepsilon}_v$ relationship is unique for CGTs and CRS tests.

For all the tests, at a given moment, the clay specimen has an average strain ε_v, an average strain rate $\dot{\varepsilon}_v$ and an average effective stress σ_v'.

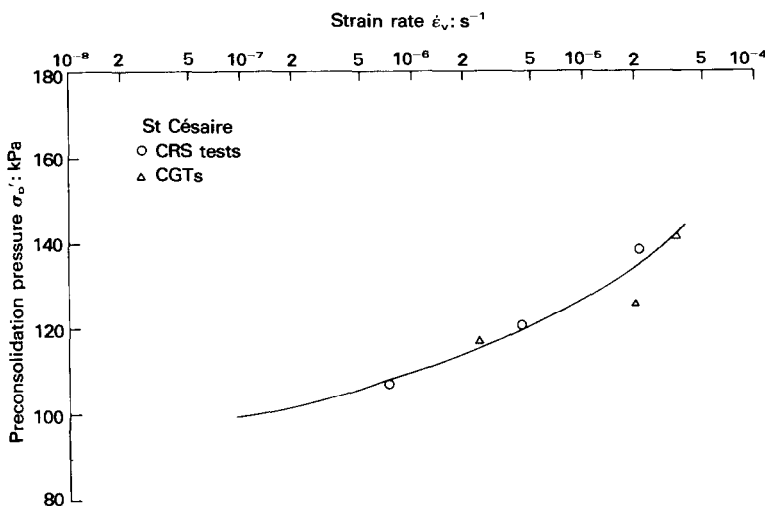**Fig. 14. Variation in preconsolidation pressure with strain rate in oedometer tests on the St Césaire clay (after Samson et al., 1981)**

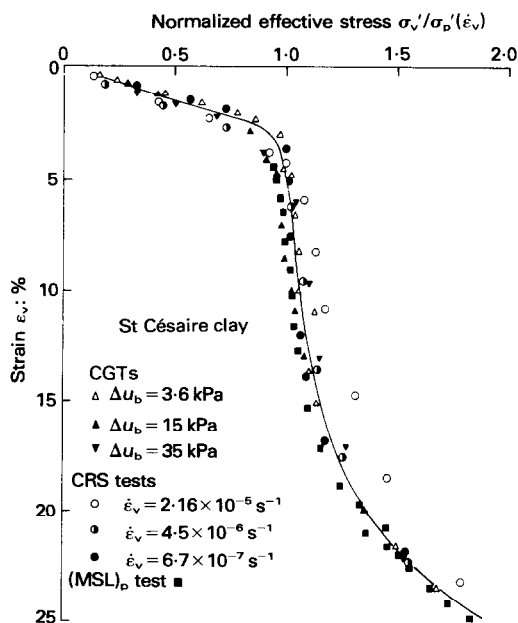Normalized effective stress $\sigma_v'/\sigma_p'(\dot{\varepsilon}_v)$

Fig. 15. Normalized effective stress–strain relationship for the St Césaire clay

It is thus possible to normalize σ_v' with respect to the preconsolidation pressure corresponding to the strain rate on the average curve drawn in Fig. 14. The results are shown in Fig. 15. Except for the CRS test carried out at a high strain rate of $2.2 \times 10^{-5}\,\mathrm{s}^{-1}$, all the results are in a very narrow range around a single line, proving again that the clay possesses, in the range of strain rates usually encountered in the laboratory, a unique stress–strain–strain rate relationship.

The existence of a unique stress–strain–strain rate relationship for natural clays supports the statements of Leroueil, Samson & Bozozuk (1983) and Leroueil, Tavenas, Samson & Morin (1983) that the preconsolidation pressure obtained in a multiple-stage loading test can be associated with the strain rate (or the domain of strain rates) measured at the end of the two or three loadings just after the preconsolidation pressure has been passed.

RHEOLOGICAL MODEL FOR NATURAL CLAYS

The experimental data presented here indicate that the rheological behaviour of natural clays may be completely described by the two equations

$$\sigma_p' = f(\dot{\varepsilon}_v) \tag{9}$$

$$\sigma_v'/\sigma_p' = g(\varepsilon_v) \tag{10}$$

Once these two relationships are known for a

given soil, any stress–strain–strain rate relationship for the soil may easily be reconstructed as shown in Fig. 16. Equations (9) and (10) may also be used directly in numerical methods to analyse consolidation problems for that soil.

Equations (9) and (10) may be combined to obtain the general rheological equation

$$\dot{\varepsilon}_v = f^{-1}\left(\frac{\sigma_v'}{g(\varepsilon_v)}\right) \tag{11}$$

Equation (11) may be experimentally defined in different ways. The method described earlier, which led to the establishment of equations (9) and (10) and the corresponding figures 7, 9, 14 and 15 for the Batiscan and St Césaire clays, derives equation (11) with reference to the preconsolidation pressures σ_p'. This approach accounts for the fact that σ_p' is a useful parameter, representative of the entire geological history of natural clays. However, this approach requires that the strain at σ_p' is approximately constant for the material considered. Equation (11) could also be determined by referring to any selected strain ε_{v0}, i.e. by defining the two relationships

$$\sigma_v'(\varepsilon_{v0}) = f'(\dot{\varepsilon}_v) \tag{12}$$

$$\sigma_v'/\sigma_v'(\varepsilon_{v0}) = g'(\varepsilon_v) \tag{13}$$

or by determining the stress–strain relation at a given strain rate $\dot{\varepsilon}_{v0}$, and generalizing in the forms

$$\sigma_v'(\dot{\varepsilon}_{v0}) = g''(\varepsilon_v) \tag{14}$$

$$\sigma_v'/\sigma_v'(\dot{\varepsilon}_{v0}) = f''(\dot{\varepsilon}_v) \tag{15}$$

From a practical point of view the experimental approach selected in this Paper, which led to equations (9) and (10) appears to be the most suitable for natural clays.

It should be kept in mind that this rheological model has a limitation at high strain rates, the stresses calculated with equation (6) being higher than expected. This was observed on the clays from Batiscan and St Césaire and on many other Champlain sea clays for strain rates greater than $1.5 \times 10^{-5}\,\mathrm{s}^{-1}$ and $du_b/d\sigma_v$ greater than 0.45. The reasons are not well understood but could be due to the method of interpretation, and in particular to unrepresentative average values of σ_v' and ε_v, and/or to a change in the rheological behaviour of the clays at high strain rates.

GENERALIZATION OF STRESS–STRAIN–STRAIN RATE RELATIONSHIP

Other eastern Canada clays

On clays from other sites of the Champlain sea basin, similar test series were performed by
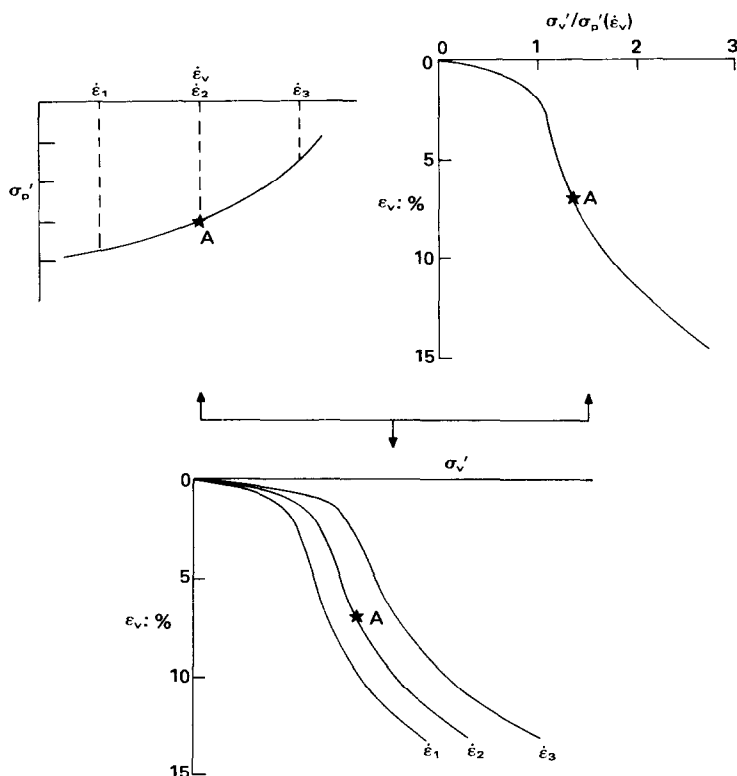
Fig. 16. Suggested rheological model for natural clays

Terratech Ltd, Montreal (Samson *et al.*, 1981), and the geotechnical section of Laval University, Quebec (Leahy, 1980). The data have been analysed and the results have been presented by Kabbaj *et al.* (1984). The behaviour was essentially the same as previously described and only typical results are shown here.

The clay from the Joliette site was sampled and tested using the same technique as for the St Césaire clay. The main properties of this clay are presented in Table 1. Its conventional preconsolidation pressure is 115 kPa. Three CRS tests ($\dot{\varepsilon}_v = 2\cdot2 \times 10^{-5}\,\mathrm{s}^{-1}$, $\dot{\varepsilon}_v = 4\cdot5 \times 10^{-6}\,\mathrm{s}^{-1}$ and $\dot{\varepsilon}_v = 6\cdot7 \times 10^{-7}\,\mathrm{s}^{-1}$), one CGT ($\Delta u_b = 10$ kPa) and two multiple-stage loading tests (one with reloading after 24 h $(\mathrm{MSL})_{24}$, and one with reloading after the end of primary consolidation $(\mathrm{MSL})_p$) were carried out. The preconsolidation pressures were associated to strain rates, as described earlier for the CGTs and the CRS tests; for the multiple-stage loading tests, the strain rate or range of strain rate was that obtained at the end of the two or three loadings just after σ_p' had been passed, as suggested by Leroueil, Samson & Bozozuk (1983) and Leroueil, Tavenas, Samson & Morin (1983). The precon-

solidation pressure–strain rate relation is shown in Fig. 17(a) while the normalized stress–strain relation $((\sigma_v'/\sigma_p')-\varepsilon_v)$ is shown in Fig. 17(b). If the variation in the preconsolidation pressure with strain rate is similar to the variations observed for the clays from Batiscan and St Césaire, the normalized stress–strain curve is much flatter, the stress necessary to reach a strain of 20% being 2·7 times the preconsolidation pressure, compared with 1·5 and 1·35 times for the clays from Batiscan and St Césaire.

The clays from the Louiseville and Mascouche sites were sampled and tested using the same technique as for the Batiscan clay. Their main properties are presented in Table 1 and their conventional preconsolidation pressures are respectively 160 kPa and 270 kPa. On both clays, series of CRS tests with strain rates varying between $5\cdot2 \times 10^{-7}\,\mathrm{s}^{-1}$ and $1\cdot8 \times 10^{-5}\,\mathrm{s}^{-1}$ and one CGT with a pore pressure difference $\Delta u_b = 15$ kPa were carried out. The preconsolidation pressure–strain rate relations are shown in Figs 18(a) and 19(a) while the normalized stress–strain relations are shown in Figs 18(b) and 19(b).

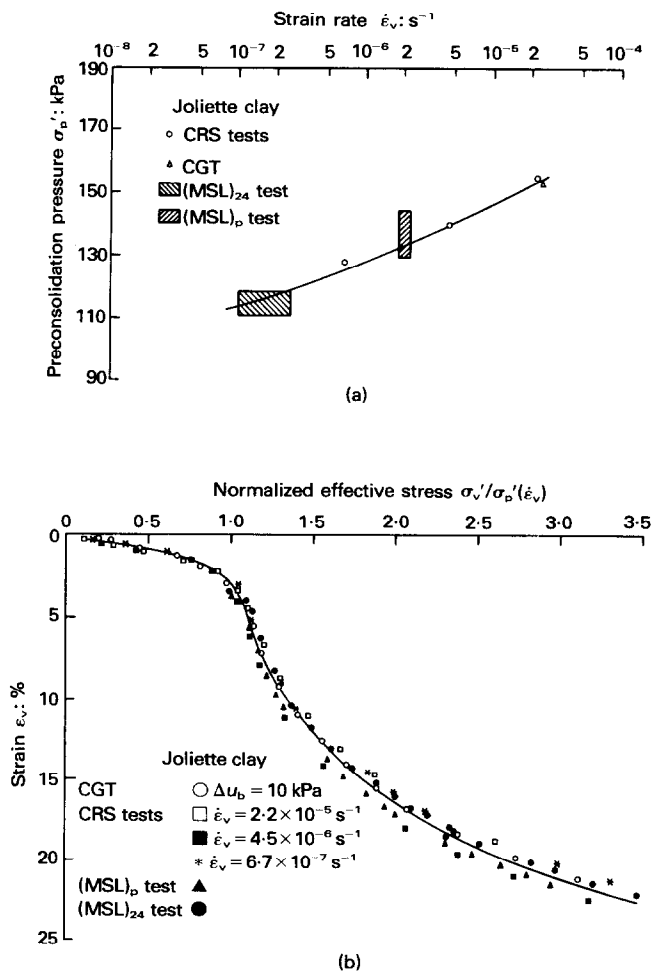The three series of test results presented in

Fig. 17. $\sigma_p' - \dot{\varepsilon}_v$ and $(\sigma_v'/\sigma_p') - \varepsilon_v$ relations for Joliette clay (after Samson *et al.*, 1981)

Figs 17–19 show very little scatter and confirm the existence for Champlain sea clays of a unique $\sigma_v' - \varepsilon_v - \dot{\varepsilon}_v$ relationship which can be expressed by equation (11).

Considering Figs 7, 14, 17(a), 18(a) and 19(a), it can be seen that the variation in the preconsolidation pressure with strain rate is very similar from clay to clay. From these results and others obtained on Champlain sea clays, Leroueil, Tavenas, Samson & Morin (1983) showed that the $\sigma_p' - \varepsilon_v$ curves can be normalized with respect to the preconsolidation pressure obtained at a reference strain rate. The results are presented in Fig. 20 where the reference strain rate is $4 \times 10^{-6} \, \text{s}^{-1}$; they indicate that the change in $\Delta\sigma_p'/\sigma_p'$ with strain rate is about the same for all Champlain sea clays.

In contrast, the $(\sigma_v'/\sigma_p') - \varepsilon_v$ curves vary markedly from clay to clay. Figs 15 and 17(b) indicate that to reach a strain of 20% at a constant strain rate an effective stress of 1·35 times the preconsolidation pressure is necessary for the clay from St Césaire, while a stress of $2·7\sigma_p'$ is needed for the clay from Joliette.

Series of special oedometer tests were also performed by other researchers on eastern Canada clays: Crawford (1965) and Vaid, Robertson & Campanella (1979) performed CRS tests, and Jarrett (1967) carried out oedometer tests in which the rate of loading was constant. In each case, the published data show a significant strain rate effect but do not allow a detailed analysis in terms of stress–strain–strain rate. However, as a first approximation, the
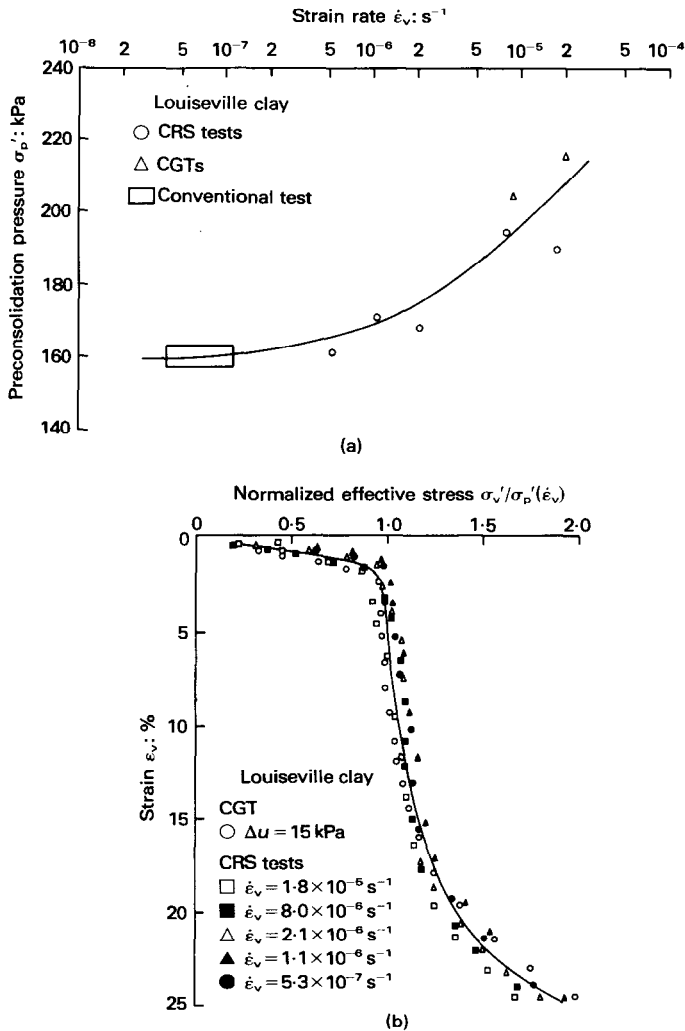
Fig. 18. $\sigma_p'-\dot{\varepsilon}_v$ and $(\sigma_v'/\sigma_p')-\varepsilon_v$ relations for Louiseville clay

stress–strain curves obtained in CRS tests by Crawford (1965) and Vaid et al. (1979) can be normalized in the manner described here.

Clays from outside eastern Canada

Series of test results obtained on clays from outside eastern Canada have also been published and can be used to verify the general validity of the model established here.

Natural clays. Sällfors (1975) carried out a series of six CRS tests on specimens of intact clay taken at a depth of 7 m at the site of Bäckebol, Sweden. The strain rates used varied between $1{\cdot}66 \times 10^{-5}\,\text{s}^{-1}$ and $5 \times 10^{-7}\,\text{s}^{-1}$. Fig. 21(a) shows the relationship between the preconsolidation pressure obtained at a strain of

about 3·5% and the strain rate. The shape is very similar to the shapes observed for Champlain sea clays. Fig. 21(b) shows points of the stress–strain curves obtained in CRS tests normalized with respect to the preconsolidation pressure obtained at the corresponding strain rate (Fig. 21(a)). The scatter of the data is very small and the rheological behaviour of the Bäckebol clay can be described by the two curves in Fig. 21 or by equation (11), following the principle established for Champlain clays.

On clay specimens from the same site of Bäckebol, but taken at a depth of 8 m, Larsson (1981) carried out eight multiple-stage loading oedometer tests with load increment ratios $(\Delta\sigma_v/\sigma_v)$ of almost unity and defined such that
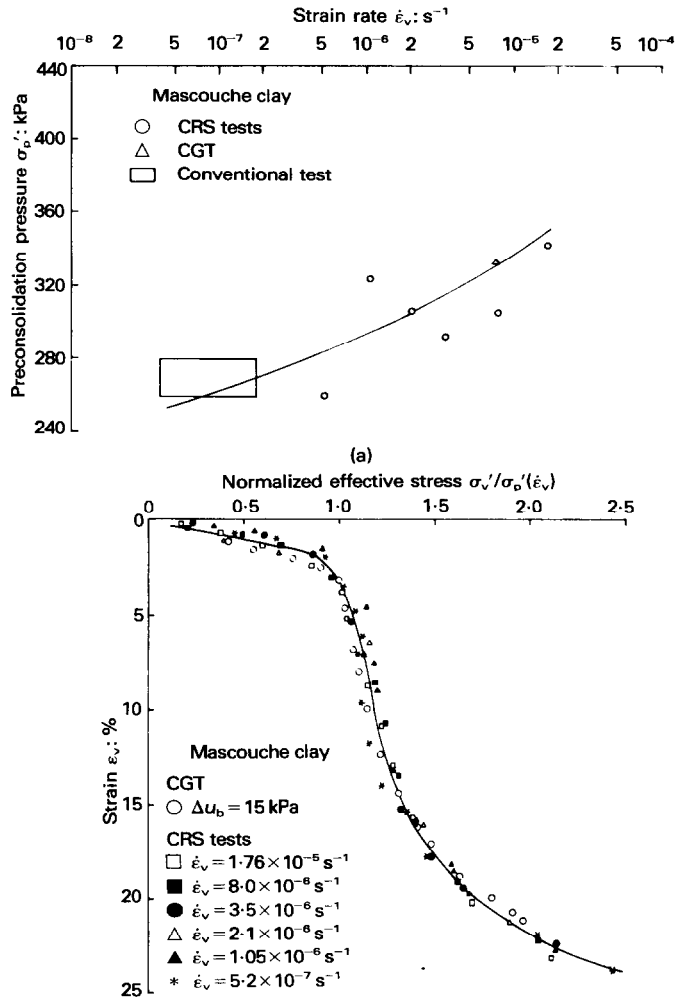
Fig. 19. $\sigma_p'-\dot{\varepsilon}_v$ and $(\sigma_v'/\sigma_p')-\varepsilon_v$ relations for Mascouche clay
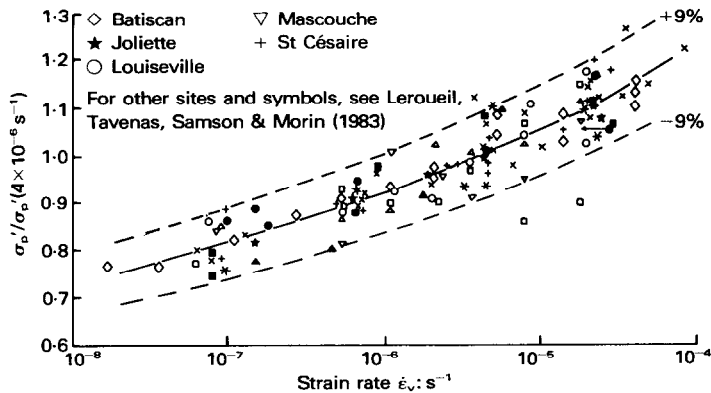

Fig. 20. Normalized preconsolidation pressure–strain rate relationship for Champlain sea clays (from Leroueil, Tavenas, Samson & Morin, 1983)
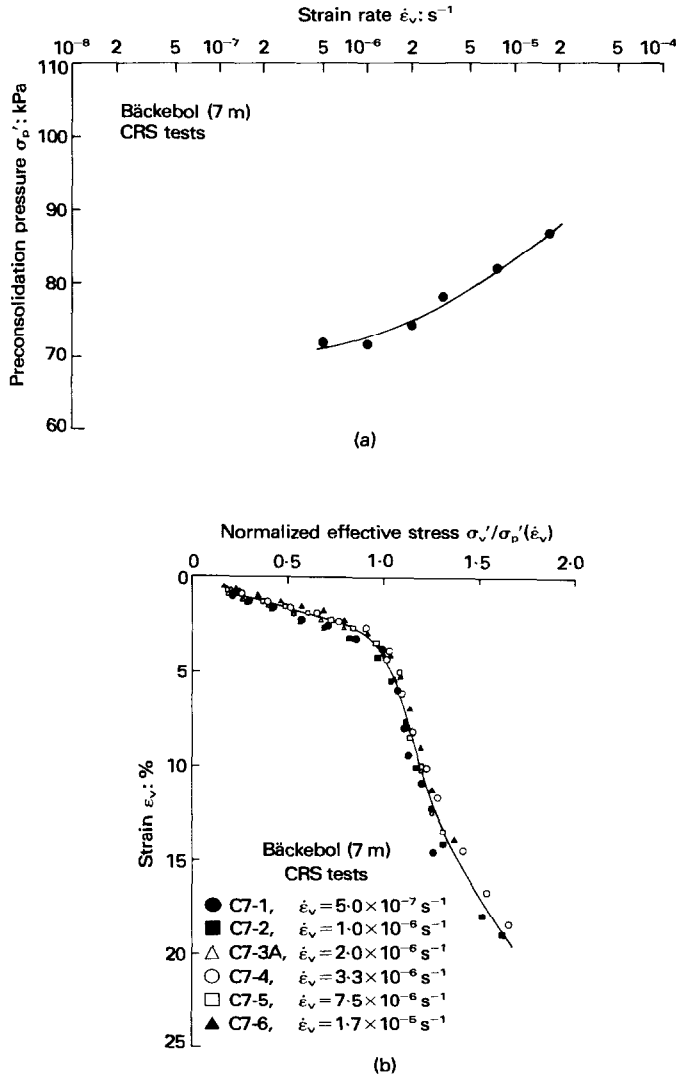
Fig. 21. $\sigma_p'-\dot{\varepsilon}_v$ and $(\sigma_v'/\sigma_p')-\varepsilon_v$ relations for Bäckebol clay at a depth of 7 m (after Sällfors, 1975)

the applied stresses were different for the eight specimens. These tests gave almost continuous stress–strain curves. In these tests, the end of primary consolidation has been obtained at strain rates higher than $10^{-6}\,s^{-1}$ and from the test results Larsson was able to draw curves corresponding to strain rates of $10^{-6}\,s^{-1}$, $10^{-7}\,s^{-1}$ and $10^{-8}\,s^{-1}$. From these curves, it was possible to estimate the preconsolidation pressures which are plotted against the strain rate in Fig. 22(a). The normalized effective stress–strain curves, drawn in Fig. 22(b), superimpose, confirming the validity of the proposed model.

A strain rate effect was also observed on a clay from Belfast, Northern Ireland, when Graham et al. (1983) performed a special CRS test in which the strain rate was changed at various strains. The same researchers reported strain rate effects on the preconsolidation pressure of various other clays from Belfast, Northern Ireland, Drammen, Norway, and Winnipeg, Canada. Whereas Graham et al. suggested a linear relationship between the preconsolidation pressure and the logarithm of strain rate, most of the published data (the average curve obtained from 14 Champlain sea clays (Fig. 20), clay from Bäckebol (Figs 21 and 22), clay from Drammen (Graham et al., 1983) and the clay
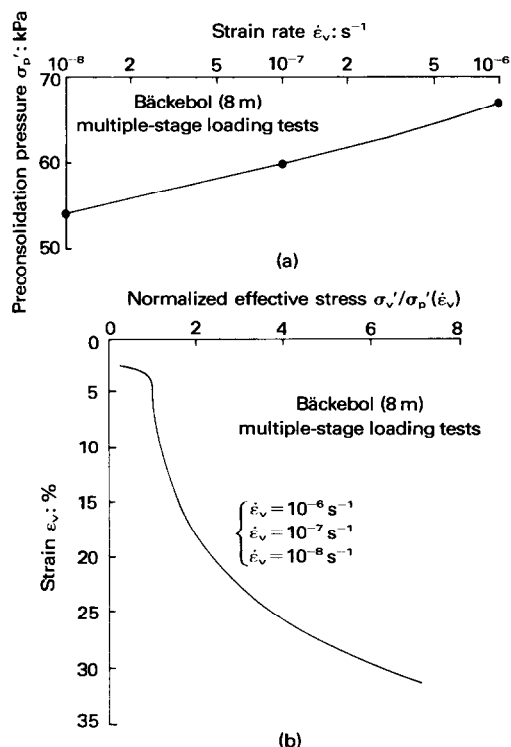
Fig. 22. $\sigma_p'-\dot{\varepsilon}_v$ and $(\sigma_v'/\sigma_p')-\varepsilon_v$ **relations for Bäckebol clay at a depth of 8 m (after Larsson, 1981)**

from St Jean-Vianney (Vaid et al., 1979)) indicate a decrease in the strain rate effect with decreasing strain rate.

Remoulded clays. Burghignoli (1979) presented results of a series of constant rate of loading oedometer tests on a remoulded clay from Fiumicino, Italy. The preconsolidation pressures were not well defined in these tests and the approach used for the natural clays, with normalization with respect to σ_p', could not be used as such. A detailed analysis of the results (Kabbaj et al., 1984) showed, however, that the rheological behaviour of the remoulded Fiumicino clay can be described by two curves corresponding to equations (14) and (15) and is thus consistent with the model proposed here.

Smith & Wahls (1969) carried out series of CRS oedometer tests on kaolinite and calcium montmorillonite. The pore pressures measured in tests on montmorillonite were as high as 88% of the applied total stress and, as indicated by Smith and Wahls, in such conditions the interpretation of the tests becomes questionable; these results have been disregarded. The results obtained on kaolinite are very different from other results since they do not present notice-

able strain rate effects. This can be considered as a particular case of the proposed model (equation (11)) in which the variation in the preconsolidation pressure (or the effective stress at a given strain or void ratio) with strain rate is negligible.

Finally, when considering remoulded clays, the behaviour represented by equation (11) may be not general since, as shown by Leonards & Altschaeffl (1964), there could be a strengthening of the bonds between particles.

DISCUSSION

In the previous sections, a rheological model for natural clays has been established. In this section, the physical meaning of this model and its practical implications will be discussed.

Significance of the proposed model

As previously shown, the rheological behaviour of sensitive natural clays is completely described by two curves ($\sigma_p'-\dot{\varepsilon}_v$ and $(\sigma_v'/\sigma_p')-\varepsilon_v$). The $(\sigma_v'/\sigma_p')-\varepsilon_v$ curve has an important physical meaning since it represents the reaction of the structure of the clay and thus its mineralogy and geological history.

The $\sigma_p'-\dot{\varepsilon}_v$ curve is representative of the capability of the clay skeleton to creep. For Champlain sea clays, Leroueil, Tavenas, Samson & Morin (1983) showed that the $\sigma_p'-\dot{\varepsilon}_v$ curves had similar shapes and could be normalized as shown in Fig. 20. For other clays with different mineralogies, other $\sigma_p'-\dot{\varepsilon}_v$ curves can be expected. However, a compilation made by Mesri & Godlewski (1977) shows that the $C_{\alpha e}/C_c$ ratio, in which $C_{\alpha e} = \Delta e/\Delta \log t$ and $C_c = \Delta e/\Delta \log \sigma_v'$ are obtained from oedometer tests, is about the same (0·04) for most non-organic natural clays. Such a constant $C_{\alpha e}/C_c$ ratio implies (Mesri & Choi, 1979) that the variation in σ_p' per logarithm cycle of time or strain rate is about the same for these materials.

For clays such as the Champlain sea clays, for which the variation in the preconsolidation pressure with strain rate is known (Fig. 20), one stress–strain curve obtained from a CRS oedometer test is sufficient to determine the $\sigma_v'-\varepsilon_v-\dot{\varepsilon}_v$ relationship of the clay considered completely.

In the model proposed, the $\dot{\varepsilon}_v = $ constant curves can be normalized with respect to the preconsolidation pressure that they define. This means that, for the two curves $\dot{\varepsilon}_v = \dot{\varepsilon}_{v1}$ and $\dot{\varepsilon}_v = \dot{\varepsilon}_{v2}$ showing the preconsolidation pressures σ_{p1}' and σ_{p2}', at a given strain the effective stresses are such that

$$\frac{\sigma_{v1}'}{\sigma_{p1}'} = \frac{\sigma_{v2}'}{\sigma_{p2}'} \qquad (16)$$
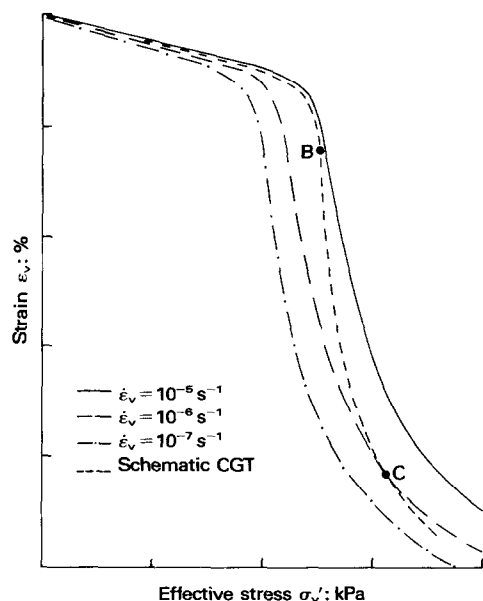
Fig. 23. Schematic state path followed during a controlled gradient oedometer test

Fig. 24. Schematic state path followed during a multiple-stage loading oedometer test

This equation can also be written as

$$\log \sigma_{v1}' - \log \sigma_{v2}' = \log \sigma_{p1}' - \log \sigma_{p2}' \quad (17)$$

which indicates that in an ε_v–$\log \sigma_v'$ diagram the distance $\log \sigma_{v1}'$–$\log \sigma_{v2}'$ between two $\dot{\varepsilon}_v =$ constant curves is a constant.

Clay response during testing

In an ε_v–σ_v' diagram such as Fig. 23, the model is depicted by a family of curves, each corresponding to a particular strain rate. At a given strain, the higher the strain rate, the higher is the effective stress. During one test, the stress–strain followed in the diagram will vary depending on the type of test and the corresponding evolution of strain rates.

In a CRS test, the soil follows an $\dot{\varepsilon}_v =$ constant curve. If the strain rate changes from $\dot{\varepsilon}_{v1}$ to $\dot{\varepsilon}_{v2}$, as for the clay from Batiscan (Fig. 6), the effective stress jumps from the $\dot{\varepsilon}_v = \dot{\varepsilon}_{v1}$ curve to the $\dot{\varepsilon}_v = \dot{\varepsilon}_{v2}$ curve.

In a CGT, the pore pressure difference between the top and the bottom of the specimen is constant and it was observed that the strain rate decreased while the strain increased in the normally consolidated range. Considering a hypothetical CGT, owing to this decrease in strain rate between points B and C (Fig. 23), the effective stress–strain curve is steeper than the curves deduced from CRS tests. This is evidenced by comparing the effective stress–strain
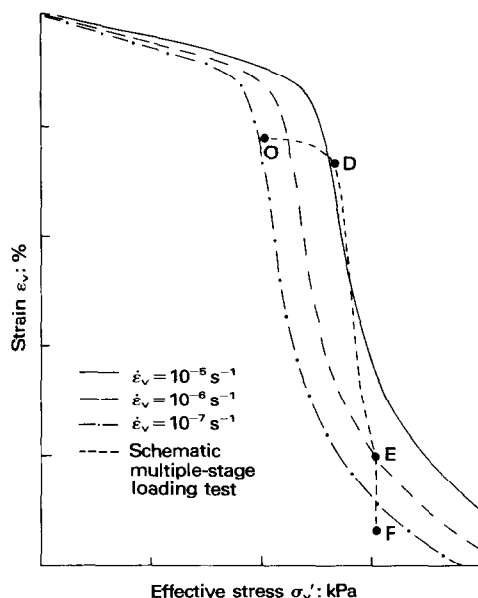
curves obtained from CRS tests (Fig. 10) and CGTs (Fig. 11(a)) on the clay from St Césaire.

In multiple-stage loading tests, the strain rate is directly related to the excess pore pressure. At the beginning of a loading period, pore pressures and thus strain rates are high and the state path lies on corresponding $\dot{\varepsilon}_v$ curves, exhibiting relatively high effective stresses. With time, the strain rate decreases and the stress–strain curve intersects the $\dot{\varepsilon}_v =$ constant curves as shown in Fig. 13 and schematically represented in Fig. 24. The behaviour is entirely controlled by two independent laws which are Darcy's law and the σ_v'–ε_v–$\dot{\varepsilon}_v$ law of the clay skeleton. Between points D and E, the strain rate is controlled by excess pore pressures and Darcy's law: this is the primary consolidation period. If the test is extended to strains in excess of ε_{vE}, when the effective stress is essentially constant, the strain rate is then controlled by the viscosity of the clay skeleton: this is the secondary consolidation period. During secondary consolidation, there are movements of porewater, and thus, according to Darcy's law, excess pore pressures. However, for small specimens these excess pore pressures are very small and almost impossible to measure (for a specimen 2 cm high with a permeability of 10^{-9} m/s, the excess pore pressure would be of the order of 0·1 kPa at a strain rate of 5×10^{-8} s^{-1}).

From the previous comments on the tests, the

values of the oedometric modulus $E_{oed} = d\sigma_v'/d\varepsilon_v$ or other strain parameters such as m_v, a_v and C_c depend on the type of test carried out to measure them.

Rheological model

To eliminate the effect of initial void ratio differences on the experimental results, the model was established by referring to strains. However, the proposed $\sigma_v'-\varepsilon_v-\dot\varepsilon_v$ relation is equivalent to a $\sigma_v'-e-\dot e$ form, i.e. to a rheological model represented by equation (4). In particular, the $\dot\varepsilon_v =$ constant curves are equivalent to the isotaches ($\dot e =$ constant) suggested by Šuklje (1957). Moreover, the tests carried out in the present study (on small specimens and in a certain domain of strain rate) do not indicate a significant influence of the stress rate $\dot\sigma_v'$ on the rheological behaviour of the clays. Consequently rheological equations of the type of equation (3) are not relevant for natural clays.

In contrast with most previous studies on the rheological behaviour of clays, no mathematical equation is suggested. The reason is that the model is completely defined by the two experimental curves corresponding to equations (9) and (10) which can be programmed in a computer, without using specific equations. However, any proposed equation should be of the general form

$$\dot\varepsilon_v = f^{-1}\left(\frac{\sigma_v'}{g(\varepsilon_v)}\right) \tag{11}$$

The model presented here is mainly based on data obtained in the normally consolidated range; the behaviour in the overconsolidated range is not as clear. The CRS tests carried out by Sällfors (1975) show separated $\dot\varepsilon_v =$ constant curves, the strain moduli $E_{oed} = d\sigma_v'/d\varepsilon_v$ decreasing with the strain rate, but this is not so evident from the CRS tests performed in the present study, the scatter in the results in the overconsolidated range being more significant. However, creep tests in the same range of stress show increases in strain with decreasing strain rates (Tavenas, Leroueil, La Rochelle & Roy, 1978, Fig. 3), indicating separated $\dot\varepsilon_v =$ constant curves. Without clear evidence of the real behaviour but accepting, to a first approximation, a normalization of the $\sigma_v'-\varepsilon_v-\dot\varepsilon_v$ behaviour (Figs 15, 17(b), 18(b), 19(b) and 21(b)), the model shown in Figs 16 and 23 with separated $\dot\varepsilon_v =$ constant curves is suggested.

The model proposed has been established on the basis of tests in which the strains were always increasing and it must be used only under such conditions; it should not be used when the clay rebounds owing to unloading or relaxes under a constant strain. In relaxation tests, the strain is constant, the strain rate is thus constant and equal to zero, and in such conditions the uniqueness of an effective stress–strain–strain rate relationship implies a constant effective stress. However, it is well known that it is not the case and that the effective stress decreases with time. When analysing this, it must be remembered that the model proposed was developed considering total strains, while the clay behaviour should probably be decomposed into elastic and plastic strain components. In the normally consolidated range, the elastic strains are small compared with the plastic strains. The model, which was developed mainly from observations in the normally consolidated range, is thus believed to represent essentially plastic strains. In the overconsolidated state, either for stresses lower than σ_p' or during relaxation, the elastic strain component could become relatively more important and the model could be representative of only part of the behaviour. There is a need for detailed research on the oedometric clay behaviour in the overconsolidated range and during relaxation.

Use and limitations

The rheological model proposed described by the two curves $\sigma_p' = f(\dot\varepsilon_v)$ and $\sigma_v'/\sigma_p' = g(\varepsilon_v)$ can be combined with a strain (or void ratio)–permeability relation (ε_v-k or $e-k$), such as those described by Tavenas, Jean, Leblond & Leroueil (1983), to resolve problems of consolidation. It should be kept in mind, however, that the model has been established on small specimens and for strain rates usually encountered in the laboratory, and thus, for the moment, it must be used only under such conditions to interpret and understand clay behaviour in the laboratory. It will probably be the basis for a reanalysis of the current practice for estimating settlements and settlement rates. However, before using this model for field applications where the strain rates are much lower and the clay layers much thicker, it is necessary to verify its validity under these conditions and in particular to determine how the $\sigma_p'-\dot\varepsilon_v$ curve extrapolates at low strain rates. A research programme on this problem is in progress at Laval University, Quebec.

CONCLUSION

Various types of oedometer tests (CRS tests, CGTs, multiple-stage loading tests and creep tests) were carried out on a variety of Champlain sea clays. From the test results a simple rheological clay model has been established. The

clay behaviour under one-dimensional compression is controlled by a unique stress–strain-strain rate relationship which can be described by only two curves $(\sigma_p'-\dot\varepsilon_v$ and $(\sigma_v'/\sigma_p')-\varepsilon_v)$. This model is a particular case of the isotache model proposed by Šuklje (1957).

From published data on secondary consolidation and strain rate effects, this model may be representative of a large variety of natural clays. However, the model has been established on specimens of small thickness in which the strain was continuously increasing, and, for the moment, it must be used only in these conditions.

REFERENCES

Aboshi, H. (1973). An experimental investigation on the similitude in the consolidation of a soft clay, including the secondary creep settlement. *Proc. 8th Int. Conf. Soil Mech. Fdn Engng, Moscow* **4**, No. 3, 88.

Barden, L. (1965). Consolidation of clay with non-linear viscosity. *Géotechnique* **15**, No. 4, 345–362.

Battelino, D. (1973). Oedometer testing of viscous soils. *Proc. 8th Int. Conf. Soil Mech. Fdn Engng Moscow* **1**, No. 1, 25–30.

Berre, T. & Iversen, K. (1972). Oedometer tests with different specimen heights on a clay exhibiting large secondary compression. *Géotechnique* **22**, No. 1, 53–70.

Bjerrum, L. (1967). Engineering geology of Norwegian normally consolidated marine clays as related to the settlements of buildings. *Géotechnique* **17**, No. 2, 83–118.

Bouchard, R. (1982). *Effet de la vitesse sur le comportement oedométrique de l'argile de Batiscan.* MSc thesis, Laval University, Quebec.

Buisman, A. S. (1936). Results of long duration settlement tests. *Proc. 1st Int. Conf. Soil Mech. Fdn Engng, Cambridge* **1**, 103–107.

Burghignoli, A. (1979). An experimental study of the structural viscosity of soft clays by means of continuous consolidation tests. *Proc. 7th Eur. Conf. Soil Mech. Fdn Engng, Brighton* **2**, 23–28.

Crawford, C. B. (1965). The resistance of soil structure to consolidation. *Can. Geotech. J.* **2**, No. 2, 90–97.

Davis, E. H. & Raymond, G. P. (1965). A non-linear theory of consolidation. *Géotechnique* **15**, No. 2, 161–173.

Gibson, R. E. & Lo, K. Y. (1961). *A theory of consolidation for soils exhibiting secondary compression.* Report No. 41, Norwegian Geotechnical Institute.

Graham, J., Crooks, J. H. A. & Bell, A. L. (1983). Time effects on the stress–strain behaviour of natural soft clays. *Géotechnique* **33**, No. 3, 327–340.

Hansen, B. (1969). A mathematical model for creep phenomena in clay. *Proc. 7th Int. Conf. Soil Mech. Fdn Engng, Mexico City*, Specialty session 12, pp. 12–18.

Hawley, J. G. & Borin, D. L. (1973). A unified theory for the consolidation of clays. *Proc. 8th Int. Conf. Soil Mech. Fdn Engng, Moscow* **1**, No. 3, 107–119.

Janbu, N., Tokheim, O. & Senneset, K. (1981). Consolidation tests with continuous loading. *Proc. 10th Int. Conf. Soil Mech. Fdn Engng, Stockholm* **1**, 645–654.

Jarrett, P. M. (1967). Time-dependent consolidation of a sensitive clay. *Bull. Am. Soc. Test. Mater* **7**, No. 7, 300–304.

Kabbaj, M., Leroueil, S. & Tavenas, F. (1984). *Développement d'une loi rhéologique représentative du comportement en laboratoire des argiles naturelles.* Internal Report, Department of Civil Engineering, Laval University, Quebec.

Koppejan, A. W. (1948). A formula combining the Terzaghi load compression relationship and the Buisman secular time effect. *Proc. 2nd Int. Conf. Soil Mech. Fdn Engng, Rotterdam* **3**, 32–37.

Ladd, C. C., Foott, R., Ishihara, K., Schlosser, F. & Poulos, H. J. (1977). Stress-deformation and strength characteristics. *Proc. 9th Int. Conf. Soil Mech. Fdn Engng, Tokyo* **2**, State of the art report, pp. 421–494.

La Rochelle, P., Sarrailh, J., Tavenas, F., Roy, M. & Leroueil, S. (1981). Causes of sampling disturbance and design of a new sampler for sensitive soils. *Can. Geotech. J.* **18**, No. 1, 52–66.

Larsson, R. (1981). *Drained behaviour of Swedish clays.* Report No. 12, Swedish Geotechnical Institute.

Leahy, D. (1980). *Contribution à l'étude du comportement oedométrique des argiles.* MSc thesis, Department of Civil Engineering, Laval University, Quebec.

Lebuis, J., Robert, J. M. & Rissmann, P. (1982). Regional mapping of landslide hazard. *Int. Symp. Landslides, Linköping*, pp. 205–262.

Leonards, G. A. (1977). *Proc. 9th Int. Conf. Soil Mech. Fdn Engng, Tokyo* **3**, Panel discussion, pp. 384–386.

Leonards, G. A. & Altschaeffl, A. G. (1964). Compressibility of clay. *J. Soil Mech. Fdns Div. Am. Soc. Civ. Engrs* **90**, SM5, 133–155.

Leonards, G. A. & Girault, P. (1961). A study of one-dimensional consolidation test. *Proc. 5th Int. Conf. Soil Mech. Fdn Engng, Paris* **1**, 213–218.

Leroueil, S. (1977). *Quelques considérations sur le comportement des argiles sensibles.* PhD thesis, Department of Civil Engineering, Laval University, Quebec.

Leroueil, S., Le Bihan, J. P. & Tavenas, F. (1980). An approach for the determination of the preconsolidation pressure in sensitive clays. *Can. Geotech. J.* **17**, No. 3, 446–453.

Leroueil, S., Samson, L. & Bozozuk, M. (1983). Laboratory and field determination of preconsolidation pressure at Gloucester. *Can. Geotech. J.* **20**, No. 3, 477–490.

Leroueil, S., Tavenas, F. & Le Bihan, J. P. (1983). Propriétés caractéristiques des argiles de l'est du Canada. *Can. Geotech. J.* **20**, No. 4, 681–705.

Leroueil, S., Tavenas, F., Samson, L. & Morin, P. (1983). Preconsolidation pressure of Champlain clays: part II—laboratory determination. *Can. Geotech. J.* **20**, No. 4, 803–816.

Lowe, J. III, Jonas, E. & Obrician, V. (1969). Controlled gradient consolidation test. *J. Soil Mech. Fdns Div. Am. Soc. Civ. Engrs.* **95**, SM1, 77–97.

Mesri, G. & Choi, Y. K. (1979). Strain rate behaviour of the Saint-Jean-Vianney clay: discussion. *Can. Geotech. J.* **16**, No. 4, 831–834.

Mesri, G. & Godlewski, P. M. (1977). Time and stress compressibility interrelationship. *J. Geotech. Engng Div. Am. Soc. Civ. Engrs* **103**, GT5, 417–430.

Morin, P., Leroueil, S. & Samson, L. (1983). Preconsolidation pressure of Champlain clays: part I, in situ determination. *Can. Geotech. J.* **20**, No. 4, 782–802.

Poorooshasb, H. B. & Sivapatham, T. (1969). Consolidation of sensitive clays exhibiting strong structural breakdown. *Proc. 7th Int. Conf. Soil Mech. Fdn Engng, Mexico City,* Specialty session 12, pp. 27–37.

Poskitt, T. J. & Birdsall, R. O. (1971). A theoretical and experimental investigation of mildly non-linear consolidation behaviour in saturated soil. *Can. Geotech. J.* **8**, No. 2, 182–216.

Sällfors, G. (1975). *Preconsolidation pressure of soft high plastic clays.* PhD thesis, Chalmers University of Technology, Gothenburg.

Samson, L., Leroueil, S., Morin, P. & Le Bihan, J. P.

(1981). *Pressions de préconsolidation des argiles sensibles.* DSS Contract 1SX79-00026. Division of Building Research of the National Research Council of Canada.

Sekiguchi, H. & Toriihara, M. (1976). Theory of one-dimensional consolidation of clays with consideration of their rheological properties. *Soils Fdns* **16**, No. 1, 27–44.

Smith, R. E. & Wahls, H. E. (1969). Consolidation under constant rates of strain. *J. Soil Mech. Fdns Div. Am. Soc. Civ. Engrs* **95**, SM2, 519–539.

Šuklje, L. (1957). The analysis of the consolidation process of the isotache method. *Proc. 4th Int. Conf. Soil Mech. Fdn Engng, London* **1**, 200–206.

Šuklje, L. (1969a). *Rheological aspects of soil mechanics.* London: Wiley–Interscience.

Šuklje, L. (1969b). Consolidation of viscous soils subjected to continuously increasing uniform load. In *New advances in soil mechanics,* Vol. 1, pp. 199–235. Praha.

Tavenas, F., Jean, P., Leblond, P. & Leroueil, S. (1983). The permeability of natural soft clays: part II, permeability characteristics. *Can. Geotech. J.* **20**, No. 4, 645–660.

Tavenas, F., Leroueil, S., La Rochelle, P. & Roy, M. (1978). Creep behaviour of an undisturbed lightly overconsolidated clay. *Can. Geotech. J.* **15**, No. 3, 402–423.

Taylor, D. W. (1942). *Research on consolidation of clays.* Series 82, Massachusetts Institute of Technology.

Taylor, D. W. & Merchant, W. (1940). A theory of clay consolidation accounting for secondary compression. *J. Math. Phys.* **19**, 167–185.

Terzaghi, K. (1923). Die Berechnung der Durchlassigkeitsziffer des Tones aus dem Verlauf der hydrodynamischen Spannungserscheinungen. *Sber. Wien. Akad. Wiss.* **132**, Nos. 3 & 4.

Vaid, Y. P., Robertson, P. K. & Campanella, R. G. (1979). Strain rate behaviour of Saint-Jean-Vianney clay. *Can. Geotech. J.* **16**, No. 1, 34–42.

Wissa, A. E. Z., Christian, J. T., Davis, E. H. & Heiberg, S. (1971). Consolidation at constant rate of strain. *J. Soil Mech. Fdns Div. Am. Soc. Civ. Engrs* **97**, SM10, 1393–1413.

Wu, T. H., Resendiz, D. & Neukirchner, R. J. (1966). Analysis of consolidation by rate process theory. *J. Soil Mech. Fdns Div. Am. Soc. Civ. Engrs* **92**, SM6, 229–248.